BOND GRAPH-BASED FAULT DIAGNOSIS STRATEGY APPLIED TO THE THREE-PHASE INDUCTION MOTOR

Brian Manuel González-Contreras[1], **José Luis Rullán-Lara**[2]

[1]Autonomous University of Tlaxcala (UAT), Faculty of Basic Sciences and Engineering
Calzada de Apizaquito s/n, Apizaco, Tlaxcala, México
[2]Autonomous University of Ciudad del Carmen, Faculty of Engineering
Av. 56 No. 4 Col. Aviación, Ciudad del Carmen, Campeche, México

brianmgc@ieee.org (Brian M. González-Contreras)

Abstract

Bond Graph has been used extensively in engineering applications for modeling and simulation of many kind of dynamical systems. Interaction between different domains can be explicitly expressed and cause-effect (causality) is well established by using this modeling tool. In this work, Bond Graph is employed for fault diagnosis in order to precisely find the fault on the system and at the same time, to well simulate the system dynamics. The methodology utilizes three principal stages (topographic search): causal graph, fault tree, and temporal causal graph. These stages are activated by qualitative values from the fault detection module when the fault appears. In order to obtain an effective fault diagnosis strategy, behavioral information about the parametric faults is employed for locating the specific fault. Sets of observations representing the abnormal state of the system are used as search templates to find a matching set in a library of known symptoms related to different abnormal system conditions (symptomatic search). In this way, an integrated strategy for faults diagnosis is proposed. All this information can be obtained from the same Bond Graph model, which allows an effective way for simulation of the treated system. The application is on the three-phase induction motor, six faults related to the winding phases are considered (short-circuit and open-circuit faults). Simulation results are presented in order to show the satisfactory results obtained.

Keywords: Fault detection, fault diagnosis, Bond Graph, three-phase induction motor, modeling and simulation.

Presenting Author's Biography

Brian M. González-Contreras. Was born in México, D.F. in 1976. He received the M.Sc. degree in Electronics Engineering from the National Center of Research and Technological Development (CENIDET), México. From 2003 he was appointed permanent lecturer at the Autonomous University of Tlaxcala. Currently he is pursuing the Ph.D. degree in the Centre de Recherche en Automatique de Nancy at Nancy University, France. Research interests are currently focused upon the design of fault tolerant control systems, fault diagnosis and modeling of engineering systems.

ISBN 978-3-901608-32-2

1 Introduction

The squirrel cage induction motor is one of the electric rotary machines most used in low, medium and high industrial applications. This machine is susceptible to fail and this represents lost of money and time for industry. Some of the widely encountered machine failures include stator winding failures, broken bars, and bearing race [1]. Therefore, the anticipated detection of possible faults allows to program its maintenance and to reduce costs on line productions.

In the Fault Detection and Diagnosis (FDD) area, there are many techniques that have been applied to the induction motor [1], [2]. Most of these methods need a high signal processing and high cost sensors. Other methods need few hardware and software effort, thus FDD is not the best but the effective and then there is a trade-off between advantages and disadvantages.

For fault diagnosis, Bond Graph (BG) has been proposed and explored since nineteen decade [3], [4]. Because BG was born as a modeling technique, few work exists in using it for FDD. However, BG is a practical technique to construct models in an unified way whatever the physical system. It shows a direct correspondence between system components and physical phenomena affecting the system. Therefore, it is relatively easy to obtain not only the model of a system but also a component fault representation. By using BG modeling in FDD methodologies, papers as [5], generates analytical redundancy relations (ARR) from a BG model based on structural and causal properties, also elimination of unknown variables from the corresponding process model is proposed. Based on causality inversion provided by the BG model, i.e., introducing process measurements as sources such that they are external nodes, a strategy is proposed in [6]. Most of authors that have employed the BG for modeling induction motors, consider the *qd* transformation [7], [8], [9]. However, when diagnosis related to the real motor is applied, only information from a different reference frame is obtained. In [10], a squirrel cage induction motor model in a direct physical correspondence is presented, but a deep diagnosis is not applied. Using this result, this paper pretends to show how the BG might be used to cope modeling, simulation and fault diagnosis aspects, in order to take advantage from the only obtained model.

In this paper, an application of the BG modeling theory in a fault diagnosis strategy is presented. This strategy starts out with the usual qualitative FDD method developed in [3], where topological search from the BG model is employed. The significance of our work is that it provides a simple and effective integrated analysis in order to simulate and to obtain an useful fault diagnosis. Our contribution is with respect to propose a modification to the original method [3] in order to be able to analyze the derivative causality involved in the motor model, by modifying the fault tree construction, and by using system's behavioral analysis when parameters fail, i.e., symptomatic search. The application is entirely in simulation (under software MATLAB$_{©}$ v7 and SIMULINK$_{©}$ v6.1) and supposes a machine working at the steady state. Although faults in a squirrel cage inductor motor may be mechanical, electrical or both of them, we consider only electrical faults, and from these, we consider short-circuit and open-circuit faults in the stator winding. It is pointed out that the strategy presented here, can diagnose other parametric faults, but we consider the latter more interesting in order to show the capability of the strategy. Related applications using the BG-based fault diagnosis proposed in [3] can be found, as a liquid-solid cooled system [4], a direct current motor [11], and a three-phase inverter [12], but there is not application in alternating current machines.

The paper is organized as follows. Section 2 contains a general overview of the BG modeling theory. The fault diagnosis approach employed in this paper is described in section 3. In section 4 the induction motor model in *qd* reference frame, and its respective BG model are presented. Then, application results are given in section 5. Finally, in section 6 conclusion is given.

2 Bond Graph Modeling

This theory has been extensively used to model multi-energy domain systems. BG technique and formulation of mathematical equations is well discussed in [13] and [14]. In this formalism there is a small and well defined set of generic physical mechanisms that are described as BG elements, which show the system interactions.

2.1 Elements

In BG terms, two sources (Se and Sf), three generalized passive elements (I, C, and R) and four constraints (*0*, *1*, TF, and GY) are used to model any energetic process. The idea is to represent the power exchange between lumped elements and to use the reference power directions as an unified coordinate system across different energy domains. Power variables are the generalized *flow* and the generalized *effort*, whose product is the power. The BG elements are:

- Energy Source: effort Se and flow Sf.
- Dissipation energy element: R.
- Storage energy elements: Capacity C relates potential energy and inertia I relates kinetic energy.
- Conversion energy elements: Transformer TF, which does proportional the effort and the flow of the same physical domain. Gyrator GY, which does the effort of one physical domain proportional to the flow of other physical domain.
- Effort junction or 0-junction: Its symbol is a zero and hold the same effort over all bonds connected to it. The algebraic sum of all flows is zero.
- Flow junction or 1-junction: Its symbol is a one and hold the same flow over all bonds connected to it. The algebraic sum of all efforts is zero.

2.2 Causality

Causality represents the sense in which variables are related as cause-effect. Graphically, the causality is represented by a stroke (*causal stroke*) that indicates, by

convention, in which way the effort is applied, and the flow being applied in the other way. In the case of Fig. 1 *a*), A imposes the effort to B and B the flow to A. The inverse case is presented in Fig. 1 *b*). For storage elements, according to the position of the causal stroke, we define the notion of integral and derivative causality. In

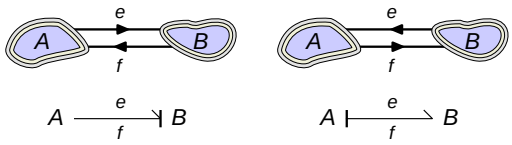

a) Causality from A to B. b) Causality from B to A.

Fig. 1 Causal stroke in Bond Graph

integral causality (preferred causality) the constitutive relation between the effort and the flow is under an integral form, and in *derivative causality* under a derivative form [14]. A procedure called Sequential Causal Assignment Procedure (SCAP) [13] allows to assign the causality to the whole BG model that then becomes a *causal* BG. SCAP is briefly enumerated as follows:

1. Choose any source (Se, Sf), and assign its required causality. Extend the causal implications through the graph as far as possible, using the constraint elements (0, 1, GY, TF). Repeat until all sources have been used.

2. Choose any storage element (C or I), and assign its preferred (integration) causality. Extend the causal implications through the graph as far as possible, using the constraint elements (0, 1, GY, TF). Repeat until all storage elements have been assigned a causality. In many practical cases all bonds will be causally oriented after this stage. In some cases, certain bonds will not yet have been assigned. Then the causal assignment is completed using the following two last steps.

3. Choose any unassigned R-element and assign a causality to it (basically arbitrary). Extend the causal implications through the graph as far as possible, using the constraint elements (0, 1, GY, TF). Repeat until all R-elements have been used.

4. Choose any remaining unassigned bond (joined to two constraint elements), and assign a causality to it arbitrarily. Extend the causal implications through the graph as far as possible, using the constraint elements (0, 1, GY, TF). Repeat until all remaining bonds have been assigned.

There are many advantages of using causality, such as systematic equation derivation and detection of equation incoherences. For 0-junction, all bonds connected to it are constrained by the junction to have the same effort value at all times, and only one of the bonds connected to the junction will set the effort value of this junction (causal stroke at the side of the junction), all other bonds will use it. In Fig. 2, effort e_4 and flow f_4

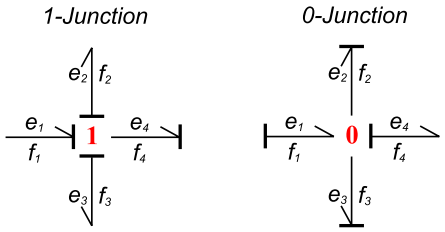

Fig. 2 Causality for the two kinds of BG junctions

are called consequent variables and the rest are precedent variables. The relationships are:

$$e_1 = e_2 = e_3 = e_4, \quad (1)$$
$$f_4 = f_1 - f_2 - f_3. \quad (2)$$

For 1-junction, the dual case of the 0-junction, all bonds connected to it are constrained to have the same flow values, this implies that only one of the bonds connected to the junction will set the flow value of this junction (causal stroke away from the junction), and all other bonds will use it. In Fig. 2, effort e_4 and flow f_4 are called consequents variables and the rest are precedent variables. The relationships are:

$$f_1 = f_2 = f_3 = f_4, \quad (3)$$
$$e_4 = e_1 - e_2 - e_3. \quad (4)$$

Readers interested on more aspects related to BG are encouraged to consult basic literature on the subject ([13], [14], and references in [3], or [11], for example).

3 Fault Diagnosis

A system that includes the capacity of detecting, isolating, identifying or classifying faults is called a fault diagnosis system [15]. The idea is to generate signals that reflect inconsistencies between the nominal and the faulty system operation. Such signals, termed *residuals* (*symptoms*), are usually generated using analytical approaches resulting from comparisons. Then, a decision procedure for diagnosis, which allows the determination of the type of fault with as many details as possible (such as the size and location), is required. Here is considered that a model of the system exists.

Model-based FDD methods require a mathematical model representing the system dynamics. According to [15] and [16], FDD methodologies can be grouped in quantitative and qualitative approaches. A FDD system should combine both numerical (quantitative) and symbolic (qualitative) information in order to be complete [15]. Use of an energy-based modeling tool such as BG to formulate equations is well established for physical systems, being a modeling methodology well suited to cover these two aspects for FDD.

3.1 Qualitative and Quantitative Approaches

Model-based methods are usually developed based on some fundamental understanding of the physics of the

process [15]. In *quantitative* models this understanding is expressed in terms of mathematical functional relationships between inputs and outputs of the system. In contrast, in *qualitative* models these relationships are expressed in terms of qualitative functions (structural and functional analysis, signed directed graphs, etc.) centered around different process units. Then a search of the fault is required.

3.1.1 Qualitative Analysis

There are fundamentally two different approaches to search in qualitative fault diagnosis [17]: topographic search and symptomatic search. *Topographic* searches perform malfunction analysis using a template of normal operation, whereas, *symptomatic* searches look for symptoms to direct the search to the fault location. A set of observations representing the abnormal state of the system can be used as a search template to find a matching set in a library of known symptoms.

3.2 Bond Graph for Qualitative FDD

In the methodology developed in [3] topographic search is employed, where search is performed in the faulty system with reference to a template representing normal or planned operation [17]. The fault will be found as a mismatch and identified by its location in the system. Note that here assumption is made only about the normal operating mode. Applications using this methodology have been successfully developed in a cooling system [4] and in a *cd* motor [11]. This methodology contains the following stages that will be applied to the induction motor. Details of each stage can be found in detail in [3], [4], or application of them in [11] and [12].

3.2.1 Causal Graph

The causal graph shows the path of a signal magnitude when a change propagates through the system elements. Signal magnitude changes are defined as qualitative values compared with nominal signal values: "+" if the signal magnitude increases, "−" if the signal magnitude decreases and "0" if the signal magnitude is constant. This graph is based on the BG model equations.

3.2.2 Fault Tree

The objective of this stage is to get a fault hypothesis set with elements that might generate the abnormal behavior, i.e., a first fault localization stage. It is propagated (in reverse way) a non admitted signal magnitude (fault) through each effort and flow variable, and through the system parameters. Each variable has a fault tree, and this begins in a measured or estimated variable which changes qualitatively $(+, -, 0)$ after a fault occurs. This change propagates through the causal graph and the possible faulty parameters are collected. This analysis gives a set of possible parameters that can be the origin of the supposed fault. Normally, when a fault occurs, a propagation of a signal magnitude change finishes when an effort or flow variable is found two times. A *change* to the original methodology in [3] *is proposed*. In this variant, *propagation finishes* when an effort or flow variable is found two times *but with a different sign* for the measured or estimated variable. Using this change to the methodology, in [12] an application to the three-phase inverter is presented.

3.2.3 Temporal Causal Graph

This stage (known as TCG) performs fault hypothesis sets reduction previously obtained from the fault tree. In a similar way as that for fault trees, a forward propagation is done but in this case is through the differentials elements: information of qualitative changes of variables and their derivatives are obtained. *Signatures*, i.e., prediction of the zero, first, and higher order time derivative effects of a system variable as qualitative values, are employed to construct the TCG's. This information is compared with the real variables and with their corresponding derivatives in order to determine the system faulty parameters. Details can be consulted in [3].

4 Three-Phase Induction Motor

The squirrel cage induction motor considered here can be found in more detail for analysis and operation purposes in [18]. For this machine, voltages and currents of both stator and rotor are changed to the arbitrary reference frame *qd* axis by means of the following transformation equations:

$$V_{qd} = \mathbf{R} I_{qd} + \Omega p \Lambda_{qd}, \tag{5}$$

where $V_{qd} = [v_{qs} \quad v_{ds} \quad 0 \quad 0]^T$, p is the differential operator, $I_{qd} = [i_{qs} \quad i_{ds} \quad i_{qr} \quad i_{dr}]^T$, $\Lambda_{qd} = [\lambda_{qs} \quad \lambda_{ds} \quad \lambda_{qr} \quad \lambda_{dr}]^T$ are the voltage source vector, the current vector and the flux vector in *qd* axis, respectively. Matrix $\mathbf{R}$=$diag(R_s, R_s, R_r, R_s)$, and:

$$\Omega = \begin{bmatrix} 0 & \omega & 0 & 0 \\ -\omega & 0 & 0 & 0 \\ 0 & 0 & 0 & (\omega - \omega_r) \\ 0 & 0 & -(\omega - \omega_r) & 0 \end{bmatrix}, \tag{6}$$

where R_s is the stator resistance, R_r is the rotor resistance, ω is the reference speed, and ω_r is the shaft rotor speed. The flux vector Λ_{qd} is defined as:

$$\Lambda_{qd} = \begin{bmatrix} L_s & 0 & M & 0 \\ 0 & L_s & 0 & M \\ M & 0 & L_r & 0 \\ 0 & M & 0 & L_r \end{bmatrix} I_{qd}, \tag{7}$$

where $M = 1.5L_m$, L_m is the mutual inductance, L_s is the stator inductance, and L_r is the rotor inductance. The instantaneous electromagnetic torque is:

$$\Gamma_e = \left(\frac{n}{2}\right)\left(\frac{P}{2}\right)(\lambda_{qr} i_{dr} - \lambda_{dr} i_{qr}), \tag{8}$$

where n is the number of phases and P is the number of poles. Dynamic characteristics of this machine relate torque and shaft speed through (9):

$$\Gamma_e = J\left(\frac{2}{P}\right)\frac{d\omega_r}{dt} + \beta\omega_r + \Gamma_L, \tag{9}$$

where J is the machine inertia and Γ_L is the applied load torque. Based on Eqs. (5)-(9), the two electric circuits shown in Fig. 3 are obtained.

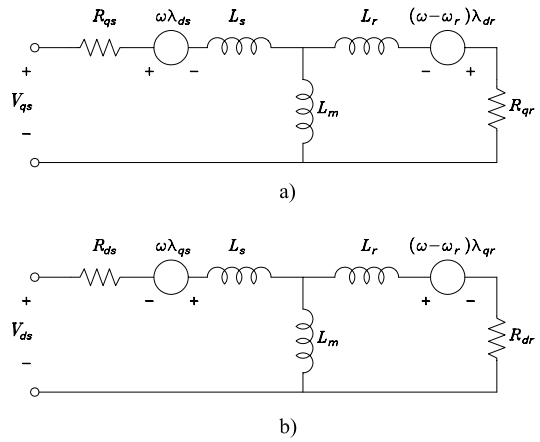

Fig. 3 a) The *q* and b) *d* equivalent circuits of symmetrical induction motor in arbitrary reference frame

4.1 Bond Graph Model

Based on the BG rules to construct a model (see §2), the circuits of Fig. 3, and the Eqs. (8)-(9), the BG model of the induction motor in the stationary reference frame is obtained (see Fig. 4). Each electric circuit has

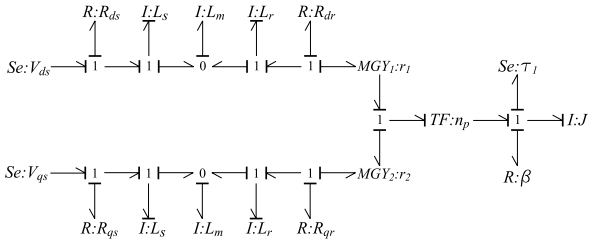

Fig. 4 Bond Graph model of three-phase induction motor in the stationary reference frame

the energy storage elements L_s, L_r and L_m interconnected. This type of connection, in the context of BG, represents a *zero causal path* [19]. This causal path is because two energy storage elements (L_s and L_r) are coupled through another energy storage element (L_m), and in order to apply the causality to the junction which connects them, a differential causality in one of the elements is presented.

Typical solutions to this problem are Lagrangian multipliers [19], singular perturbations [3] and the I-fields [8], [10], [14]. Lagrangian multipliers and singular perturbations modify the model structure by including additional elements without physical interpretations (R or C, principally) to change causality at the adjacent junctions, and therefore, causality in the storage elements. I-field is a mathematical artifice which preserves all physical elements and does not include additional elements as the other methods [8], [14]. The idea is to redraw bonds of the storage elements in such a way that they can be connected to the rest of the bonds through only two bonds. Consequently, I-fields are input-output relations between flow and effort variables. The resulting BG model of the three-phase induction motor

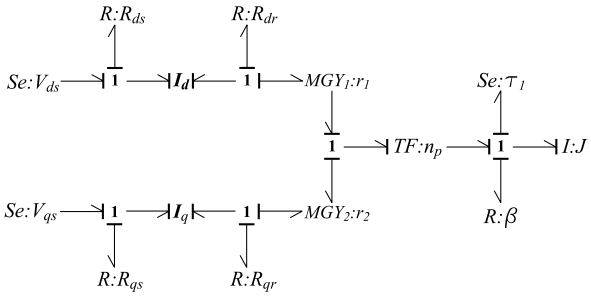

Fig. 5 Bond Graph model of the three-phase induction motor in the stationary reference frame with I-fields

using the I-fields is shown in Fig. 5. However, this model is not appropriate to develop a fault diagnosis in a real physical correspondence because any change is reflected in the *qd* frame not in *abc* frame. Thus, this fact implies two things: firstly, it is necessary to include the coordinate transformation in the model, and secondly, if this coordinate transformation has a BG representation, it must preserve the amplitude and power. Fortunately, both conditions can be carried out. The coordinate transformation [9] is:

$$\begin{bmatrix} v_q \\ v_d \end{bmatrix} = \begin{bmatrix} \sqrt{\frac{2}{3}} & -\frac{1}{\sqrt{6}} & -\frac{1}{\sqrt{6}} \\ 0 & \frac{1}{\sqrt{2}} & -\frac{1}{\sqrt{2}} \end{bmatrix} \begin{bmatrix} v_a \\ v_b \\ v_c \end{bmatrix}. \quad (10)$$

Equation (10) has a BG representation and it is included in the BG model in order to obtain the model depicted in Fig. 6. The transformers TF_1-TF_5 achieve the coor-

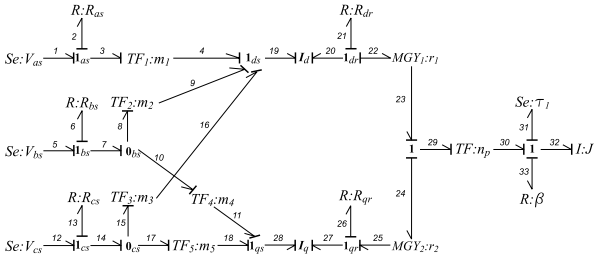

Fig. 6 Bond Graph model of the three-phase induction motor including Eq. (10) and I-fields

dinate transformations by means of:

$$\begin{aligned} m_1 &= \sqrt{3/2},\ m_2 = m_3 = -\sqrt{6}, \\ m_4 &= \sqrt{2}, \quad m_5 = -\sqrt{2}. \end{aligned} \quad (11)$$

For the gyrators it is taken:

$$r_1 = L_m f_{28} + (L_r + L_m) f_{27}, \quad (12)$$
$$r_2 = L_m f_{19} + (L_r + L_m) f_{20}, \quad (13)$$

and for the transformer of the mechanical part:

$$n_p = 2/p. \quad (14)$$

This model has seven electrical output variables, three are physically measured (three stator currents: i_{as} (f_3),

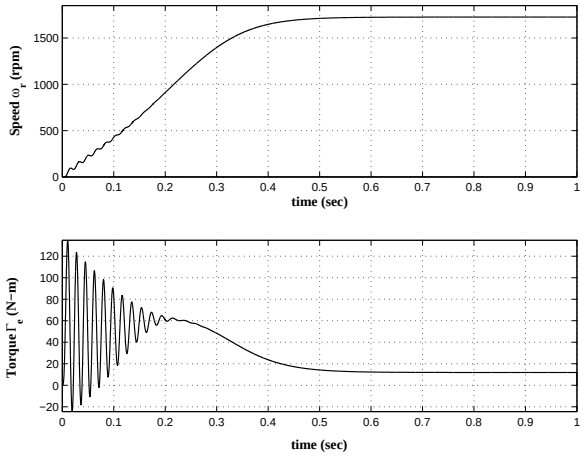

Fig. 7 Shaft speed $\omega_r(f_{32})$ (top) and torque Γ_r (bottom)

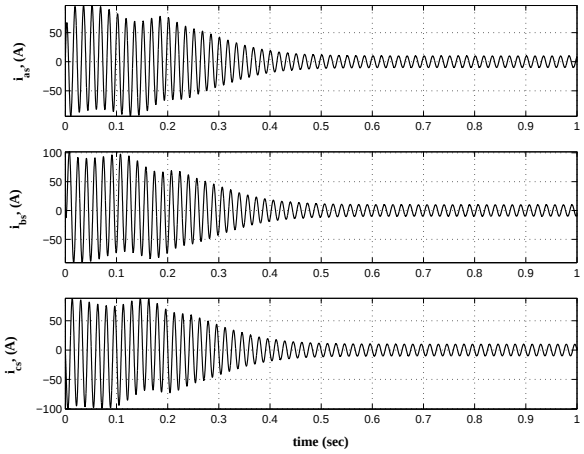

Fig. 8 Stator currents i_{as}, i_{bs} and i_{cs}

i_{bs} (f_7), i_{cs} (f_{14})), and one mechanical output variable: the shaft speed ω_r (f_{32}), also measured.

In order to validate this model for simulation (cf. [18]), Fig. 7 shows the shaft speed and torque, whereas Fig. 8 shows the three stator currents. Simulations correspond to a machine with the following physical parameters values [18]: 3 hp, 4 poles, 220 V, 60 Hz, $R_s = 0.435\,\Omega$, $R_r = 0.816\,\Omega$, $X_{ls} = X_{lr} = 0.754\,\Omega$, $X_m = 26.13\,\Omega$, β=0.089 $N \cdot m \cdot s$, τ_l=10 $N \cdot m$ and $J = 0.089\,kg \cdot m^2$, and to simplify the application, without loss of generality, it is considered that $R_s = R_{as} = R_{bs} = R_{cs}$, and $R_r = R_{dr} = R_{qr}$.

5 Application Results

All results, obtained by simulation, consider open-loop operation. The fault diagnosis strategy is only focused on the electric part of the motor.

5.1 Fault Scenarios

Six faults on the stator winding are defined as follows:

F_1- Open-circuit fault on the stator phase winding A.
F_2- Open-circuit fault on the stator phase winding B.
F_3- Open-circuit fault on the stator phase winding C.
F_4- Short-circuit fault on the stator phase winding A.
F_5- Short-circuit fault on the stator phase winding B.
F_6- Short-circuit fault on the stator phase winding C.

Only unique, abrupt and permanent short-circuit and open-circuit faults in the stator winding are treated in this paper. The faults are generated by introducing abrupt changes in the stator resistance value when the machine *operates at steady state condition*. For an open-circuit fault the respective resistance increases in 1000% and for a short-circuit fault the respective resistance decreases in 90%.

5.2 Simulation results

As example, dynamic behavior of stator currents when fault F_1 occurs at time 1 second (when steady state has been reached), is shown in Fig. 9. In the left subplots of this figure, normal values are presented. For fault detection, root mean square (rms) values of currents, and shaft speed are employed as measured signals. These values are presented in the right subplots of Fig. 9. Calculation of signal derivatives is carried out by means of state variable filters [15]. In order to detect the fault, a change beyond 1% in the nominal stator currents, and a change beyond 5% in the nominal shaft speed are used as thresholds. For fault F_1, magnitude of i_{as} current decreases drastically to zero and both stator currents, i_{bs} and i_{cs}, increase close to 190% from their steady state values. Fig. 10 shows rms and qualitative values when fault F_1 occurs (at time 1 second). The right side of this figure presents only qualitative values ($-$, 0, $+$) for the measured variables in the fault scenarios. These values are collected and resumed in Tab. 1. For example, when fault F_1 occurs, current i_{as} decreases and i_{bs} increases, and so on for the other measured variables.

5.3 Fault Diagnosis Results

There are conditions that avoid to apply directly the methodology proposed in [3]:

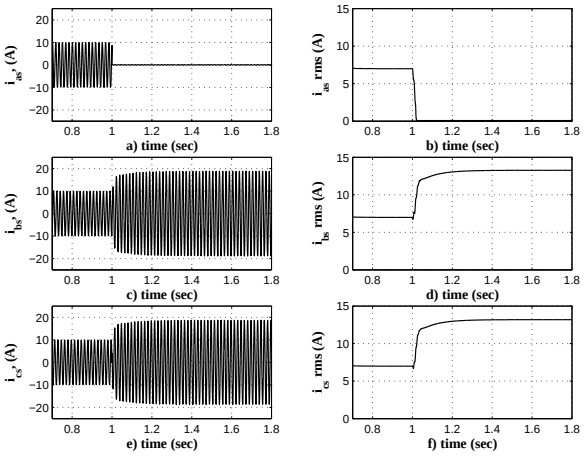

Fig. 9 Stator currents when open-circuit fault in the phase winding A occurs: a) i_{as}, b) i_{as}^{rms}, c) i_{bs}, d) i_{bs}^{rms}, e) i_{cs}, f) i_{cs}^{rms}

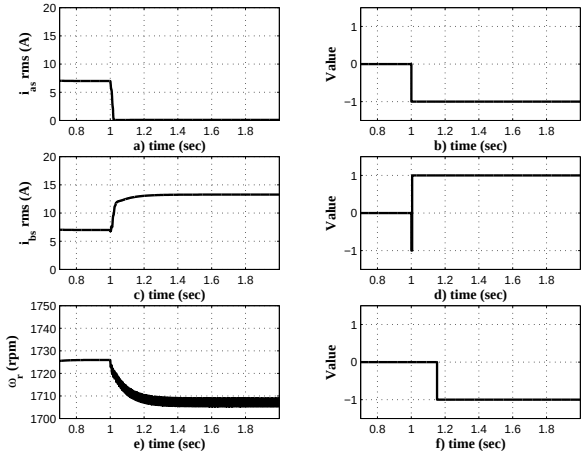

Fig. 10 Rms and qualitative values when open-circuit fault in the phase winding A occurs: a) i_{as}, b) Qualitative value for i_{as}, c) i_{bs}, d) Qualitative value for i_{bs}, e) ω_r, f) Qualitative value for ω_r

Tab. 1 Fault signatures

Fault	i_{as}	i_{bs}	i_{cs}	i_{ds}	i_{dr}	i_{qs}	i_{qr}	ω_r
F_1	-	+	+	-	-	+	+	-
F_2	+	-	+	+	+	+	+	-
F_3	+	+	-	+	+	+	-	-
F_4	+	-	+	+	-	-	-	0
F_5	+	+	-	+	+	-	-	0
F_6	-	+	+	-	-	+	+	0

- Not all the storage elements in the BG model are in integral causality even using *I*-fields.
- Not all states of the system are observable because the model includes a section of stator resistance in the *abc* reference frame and the rest of electric variables in the *qd* reference frame.

These conditions give empty fault hypothesis sets (see second column of Tab. 2), thus the variant to the original methodology [3] to construct fault trees, depicted in section 3.2.2, is applied. Under this approach the resultant fault hypothesis sets obtained from fault trees are shown in the third column of Tab. 2. Since the number of elements of these sets is greater than one, the temporal causal graph is used to reduce them. Nevertheless, the temporal causal graph could not refine these sets. Similar problems are presented in [4] and [20].

Based on the conditions and problems presented in the two last stages of the methodology, and in order to reduce the fault hypothesis sets, it is employed the structured knowledge from the BG model and the one provided by the *behavior* of the faulty process. It takes advantage from the underlying physical laws known in analytical form of the BG model in order to reconstruct the fault-symptom chains from the measured data, i.e., information from output variables in the fault scenarios. This search of faults is also known as *symptomatic* search (see 3.1.1). For the three open-circuit faults a unique behavior pattern for each case is presented:

- Current magnitude through the short-circuited winding decreases to zero, and the other current values increase.
- Shaft speed magnitude decreases in the three cases.

For this type of fault, a current increasing in each winding is because the winding resistance increases. Therefore, in the fault hypothesis sets (third column of Tab. 2) each winding resistance has the qualitative value "$+$" and the adjacent winding resistance has the qualitative value "$-$". Since the shaft speed decreases in the three open-circuits faults and the rest of parameters belong to the equivalent *qd* reference frame, we discard all parameters except parameters R_{as}^{+}, R_{bs}^{+} and R_{cs}^{+}.

For the three short-circuit faults we have the behavior described as follows:

- Shaft speed value is constant.
- Current i_{bs} decreases and currents i_{as} and i_{cs} increase for a fault in the phase winding A.
- Current i_{cs} decreases and currents i_{as} and i_{bs} increase for a fault in the phase winding B.
- Current i_{as} decreases and currents i_{bs} and i_{cs} increase for a fault in the phase winding C.

A short-circuit fault implies that a winding resistance decreases. Viewing the third column of Tab. 2, for each short-circuit fault, two resistances have decreasing values: the winding resistance when the fault occurs and the adjacent winding resistance. Taking into account the behavioral information of the variables described above, we discard parameters of the adjacent winding and the rest of parameters in each set. Fourth column of Tab. 2 shows the final results of fault diagnosis. Each fault hypothesis set is reduced to only one element, which is the parameter causing the fault. Further details of this application can be consulted in [21].

6 Conclusion

In this paper, a qualitative strategy for fault diagnosis based on Bond Graph modeling has been applied to the three-phase induction motor. The strategy involves causal graph, fault tree and temporal causal graph as the principal stages for diagnosis (topographic search), but due to the structure of the motor model (derivative causality, nonlinear relationships), has been employed behavioral information provided by analysis of the faulty system (symptomatic search) in order to obtain an effective fault diagnosis. Contribution of this paper is to propose a fault diagnosis strategy that combines fault searching approaches through the Bond Graph model, in order to cope both simulation and diagnosis aspects.

Three short-circuit and three open-circuit faults have been considered in the application, in order to show the effectiveness of the Bond Graph model not only for

Tab. 2 Fault hypothesis sets

Fault	Conventional fault tree methodology	Modified fault tree methodology	Obtained parameters
F_1	$\emptyset$	$\{R_{as}^+, R_{bs}^-, R_{cs}^-, R_{dr}^+, R_{qr}^-, \beta^+, J^-\}$	$\{R_{as}^+\}$
F_2	$\emptyset$	$\{R_{as}^-, R_{bs}^+, R_{cs}^-, R_{dr}^-, J^-\}$	$\{R_{bs}^+\}$
F_3	$\emptyset$	$\{R_{as}^-, R_{bs}^-, R_{cs}^+, R_{dr}^-, R_{qr}^+, \beta^+, J^-\}$	$\{R_{cs}^+\}$
F_4	$\emptyset$	$\{R_{as}^-, R_{bs}^+, R_{cs}^-, R_{dr}^+\}$	$\{R_{as}^-\}$
F_5	$\emptyset$	$\{R_{as}^-, R_{bs}^-, R_{cs}^+, R_{dr}^-\}$	$\{R_{bs}^-\}$
F_6	$\emptyset$	$\{R_{as}^+, R_{bs}^-, R_{cs}^-, R_{dr}^+, R_{qr}^+\}$	$\{R_{cs}^-\}$

simulation but also for fault diagnosis. This strategy gives insight about application to other systems with similar characteristics, such as induction motors and power converters related to these systems.

Acknowledgment

B.M. González-Contreras thanks PROMEP scholarship by the financial support provided through the Autonomous University of Tlaxcala, under contract UATLAX-175, PROMEP/103.5/04/1525.

7 References

[1] P. Harihara, K. Kim, and A. Parlos. Signal-based versus model-based fault diagnosis a trade-off in complexity and performance. In *SDEMPED*, pages 277–282. IEEE, 2003.

[2] A. Bonnet and G. Soukup. Cause and analysis of stator and rotor failures in three-phase squirrel-cage industrial motors. *IEEE Trans. on Industry Applications*, 28(4), 1992.

[3] P.J. Mosterman and G.Biswas. Diagnosis of continuous valued systems in transient operating regions. *IEEE Trans. on Systems, Man and Cybernetics: Part A*, 29(6):554–565, 1999.

[4] E. Manders, G. Biswas, and P. Mosterman. Signal interpretation for monitoring and diagnosis: A cooling system testbed. *IEEE Trans. on Instrument and Measurement*, 49(3):503–508, 2000.

[5] B. Ould Bouamama, K. Medjaher, M. Bayart, A.K. Samantaray, and B. Conrard. Fault detection and isolation of smart actuators using bond graphs and external models. *Control Engineering Practice*, 2(13):159–175, 2005.

[6] B. Ould Bouamama, K. Medjaher, A.K. Samantaray, and M. Staroswiecki. Supervision of an industrial steam generator. part 1: Bond graph modelling. *Control Engineering Practice*, 3(14):71–83, 2006.

[7] S. Junco. Modelización y análisis no lineal de la máquina de inducción mediante bond graphs vectoriales de potencia. *Revista Electrónica, Fac. de Ciencias Exactas, Ing. y Agrimesura*, 1(3), 1999.

[8] D. Karnopp. Understanding induction motor state equations using bond graphs. In *Int. Conf. on Bond Graph, Modelling, and Simulation*, pages 269–273, 2003.

[9] D. Sahm. A two-axis bond graph model of the dynamics of synchronous electrical machines. *J. of the Franklin Institute*, 308(3):205–218, 1979.

[10] J. Kim and M. Bryant. Bond graph model of a squirrel cage induction motor with direct physical correspondence. *Journal of Dynamic Systems, Measurement and Control*, 122:461–469, 2000.

[11] B.M. González-Contreras. Diagnóstico de fallas en un motor de corriente directa usando el método de bond graph. *M.Sc. Thesis CENIDET*, 2002.

[12] B.M. González-Contreras, J.L. Rullán-Lara, L.G. Vela-Valdés, and A. Claudio-S. Modelling, simulation and fault diagnosis of the three-phase inverter using bond graph. In *IEEE International Symposium on Industrial Electronics ISIE'07*, pages 130–135, 2007.

[13] Peter Gawthrop and Lorcan Smith. *Metamodelling: Bond graphs and dynamics systems*. Prentice Hall, London, 1996.

[14] D.C. Karnopp and R. Rosenberg. *Systems Dynamics: A Unified Approach*. Wiley Interscience, New York, 2nd edition, 2000.

[15] Rolf Isermann. Model-based fault-detection and diagnosis - status and applications. *Annual Reviews in Control*, (29):71–85, 2005.

[16] V. Venkatasubramanian, R. Rengaswamy, and S.N. Kavuri. A review of process fault detection and diagnosis. part 1: Quantitative model-based methods. *Computers and Chemical Engineering*, (27):293–311, 2003.

[17] V. Venkatasubramanian, R. Rengaswamy, and S.N. Kavuri. A review of process fault detection and diagnosis. part 2: Qualitative models and search strategies. *Computers and Chemical Engineering*, (27):313–326, 2003.

[18] P. C. Krause, O. Wasybczuk O., and S. D. Sudhoff. *Analysis of electric machinery and drives systems*. IEEE Press, New York, 2002.

[19] R. Cacho, J. Felez, and C. Vera. Deriving simulation models from bond graphs with algebraic loops. the extension to multibond graph systems. *J. of the Franklin Institute*, 337:579–600, 1992.

[20] E. Manders and G. Biswas. Fdi of abrupt faults with combined statistical detection and estimation and qualitative fault isolation. In *IFAC SAFEProcess*, pages 347–355, 2003.

[21] J. L. Rullán-Lara. Diagnóstico de fallas en la máquina de corriente alterna utilizando bond graph. *M.Sc. Thesis CENIDET*, 2006.

